Flexible cotton-AuNP thread electrode for non-enzymatic sensor of uric acid in urine

Kanyapat Teekayupak
Chulalongkorn University
Nipapan Ruecha
Chulalongkorn University
Orawon Chailapakul
Chulalongkorn University
Nadnudda Rodthongkum (Nadnudda.r@chula.ac.th)
Chulalongkorn University https://orcid.org/0000-0002-0379-5166

Research Article

Keywords: Gold nanoparticle, Cotton thread, Flexible electrode, Non-enzymatic sensor, Uric acid

Posted Date: April 23rd, 2021

DOI: https://doi.org/10.21203/rs.3.rs-427183/v1

Abstract

We report on the development of an electrochemical sensor platform based on modified cotton fibers for the non-enzymatic detection of uric acid (UA), an important biomarker for gout disease. To create the flexible electrode, a cotton thread was coated with carbon ink followed by the electrodeposition of AuNPs. Then, differential pulse voltammetry (DPV) was used to evaluate the sensor performances, and a linear detection range between 10 μM and 5.0 mM of uric acid was obtained. The sensor has a low detection limit of 0.12 μM, which is optimal for use in the patients suffering from gout disease which commonly experience concentrations of uric acid in urine higher than 4.46 mM. Furthermore, we found that the detection sensitivity of the platform was not affected by the presence of other physiological compounds present in human urine. The described platform has the potential for integration in a diaper hence enabling rapid detection and screening for gout disease.

1. Introduction

Non-invasive diagnosis allows for the direct detection of target biomarkers from body fluids without the common pain and infection risk associated with blood-based protocols (Li et al. 2019; Michelena et al. 2019; Eftekhari et al. 2019; Doménech-Carbó et al. 2018). Various substrates have been used for non-invasive diagnosis including tattoos (Bandodkar et al. 2013; Jia et al. 2013), paper-based sensors (Anastasova et al. 2017), stretchable elastomers (Martin et al. 2017) and textile substrates (Liu and Lillehoj 2017). Textiles have become an attractive material owing to their flexibility, biocompatibility and high-water absorption (Caldara et al. 2016; Promphet et al. 2019; Ren et al. 2017). Among textile-based sensors, fabric platforms usually require of a high volume of biofluid sample, while yarns and threads require of low sample volumes and offer unique microfluidic properties (Ahmed et al. 2019; Reches et al. 2010; Oliveira et al. 2019; Liu et al. 2018; Polanský et al. 2017; Weng et al. 2019).

Uric acid (UA), chemically designated as 2, 6, 8-tryhydroxypurine, is a major product of the catabolism of purine nucleosides, adenosine and guanosine. The normal concentration of uric acid in human urine varies between 1.4–4.46 mM and values higher than 4.46 mM are used for gout disease diagnosis (Azmi et al. 2015; Liu et al. 2019; Yang et al. 2018).

Non-invasive sensors of UA in human urine have been recently developed (Bai et al. 2017; Yang et al. 2018), and various techniques, such as liquid chromatography (Li et al. 2015), capillary electrophoresis (Pormsila et al. 2009), and fluorescence spectroscopy (Azmi et al. 2018) have been used for UA detection. However, while these techniques offer high sensitivity and precision, they also have some limitations such as high cost, and the requirement of highly trained personnel. An electrochemical sensor offers an alternative approach owing to its simplicity, miniaturization, rapid response and low cost (Liu et al. 2012; da Cruz et al. 2017; Income et al. 2019). Traditionally, the sensing of UA is performed via an enzymatic reaction using uricase. Although enzyme-based sensors provide high specificity and sensitivity, they have some major disadvantages, including high cost, operational complexity and low stability (Arora et al. 2014).

Non-enzymatic UA sensors based on oxidation processes occurring on electrodes have been developed (Income et al. 2019). However, non-enzymatic sensors require of high surface areas for accurate detection. Metal nanoparticles have been utilized for the surface modification of electrodes owing to their high conductivity, large surface area, high mechanical strength, and electrocatalytic properties (Yukird et al. 2018; Ji et al. 2018; Wang et al. 2018; Wang et al. 2016; Ruecha et al. 2017).

In this manuscript, we report on the development of an electrochemical sensor for the non-enzymatic detection of UA using cotton threads as flexible substrates. We coated the cotton threads with a conductive carbon ink and then electrodeposited AuNPs to increase the sensor's surface area and its electrochemical sensitivity to UA. The performance of the sensor was systematically investigated and tested in real human urine samples.

2. Material And Methods

2.1 Chemicals and materials

Uric acid (UA), potassium ferricyanide ($K_3[Fe(CN_6)]$), potassium ferrocyanide ($K_4[Fe(CN_6)]$) and gold (III) chloride trihydrate ($HAuCl_4 \cdot 3H_2O$) were purchased from Sigma–Aldrich (St. Louis, MO, USA). Silver/silver chloride (Ag/AgCl; C2130809D5) and carbon ink (C2030519P4) was obtained from Gwent group (Torfaen, United Kingdom). The carbon ink is composed of a solid carbonaceous component (*e.g.* carbon and graphite) and an epoxy resin (*e.g.* thermoplastic resin and some other additives). Potassium dihydrogen phosphate (KH_2PO_4), disodium hydrogen phosphate (Na_2HPO_4), sodium chloride (NaCl), potassium chloride (KCl) and sulphuric acid (H_2SO_4) were obtained from Carlo Erba Reagenti-SDS (Val de Reuil, France). All solutions were prepared using purified water (Millipore, USA, $R \geq 18.2$ MΩ cm^{-1}). A Phosphate buffered saline solution (PBS, 0.1 M pH 6.0) was prepared by dissolving 1.42 g Na_2HPO_4, 1.36 g KH_2PO_4, 0.58 g NaCl and 0.74 g KCl in 100 mL of high purified water. A stock solution of UA was freshly prepared in 0.1 M PBS. All chemicals were used as received.

2.2 Apparatus

The morphology and elemental composition of the cotton thread sensor were characterized by scanning electron microscopy (SEM) with energy dispersive X-rays spectroscopy (EDX) (JSM-6400; Japan Electron Optics Laboratory Co., Ltd., Tokyo, Japan). Electrochemical measurements were performed using cyclic voltammetry (CV) and differential pulse voltammetry (DPV) modes on a CHI1240B (CH Instruments, Inc., Austin, TX, USA) potentiostat, controlled with CHI1240B software. Laser desorption/ionization mass spectrometer (LDI-MS; Autoflex III MALDI-TOF MS; Bruker, MA, USA) with 25% N_2 laser intensities at 337 nM and 40 shots was used to validate the concentration of uric acid in the samples.

2.3 Sensor design

The fabrication of the cotton thread sensor is shown in Scheme 1. Firstly, a cotton thread (DMC special 25, 100% cotton B5200) was soaked in the prepared carbon ink (C2030519P4), passed through a pinhole

of a needle to remove the excess ink and obtain uniformed carbon coating on the thread, and baked at 60°C for 30 min. The carbon-coated cotton thread was used as a working electrode (WE) for all experiments. To fabricate the counter and reference electrodes of an electrochemical sensor, carbon ink (C2030519P4) was screen-printed on a polyvinylchloride (PVC) substrate and heated at 60°C for 30 min. After heating, Ag/AgCl ink (C2130809D5) was screen-printed on the same PVC substrate, dried at 60°C for 30 min, and used as a reference electrode (RE). After obtaining screen-printed electrode (SPE) template on PVC containing the RE and CE, a transparent film was punched in a hole diameter of 6 mm and attached on the as prepared SPE template using double-sided tape for creating electrochemical testing zone and hydrophobic barrier, which limit the sample area contacting with three electrodes on SPE. The carbon-coated cotton thread was placed between the RE and CE. Gold nanoparticles (AuNPs) were electrodeposited on the WE, by dropping 40 µL of 3.0 mM $HAuCl_4 \cdot 3H_2O$ followed by the applied potential of −0.6 V (vs. Ag/AgCl) for 120 s (Charoenkitamorn et al. 2015). The AuNPs modified cotton thread was carefully rinsed with purified water and dried at 60°C for 1 h prior to use.

2.4 SEM Imaging

The surface morphology of the cotton thread was observed using scanning electron microscopy (SEM). A dried sample was mounted directly on to a specimen stub, and imaging was carried out under high vacuum with an accelerated voltage of 10.0 kV using a magnification of 20,000×.

2.5 Electrochemical measurements

Electrochemical measurements were performed on a potentiostat using cyclic voltammetry (CV) and differential pulse voltammetry (DPV). The cotton thread electrode was electrochemically characterized using a standard solution of 5.0 mM $[Fe(CN)_6]^{3-/4-}$ via CV with a potential ranging from −1.2 V to + 0.9 V and a scan rate of 100 mV/s. During UA determination procedures, DPV measurements were performed using a potential from −0.3 V to + 0.8 V with a step potential of 15 mV, an amplitude of 200 mV and a pulse width of 50 ms.

2.6 Sample collection and sample preparation

A standard calibration curve, obtained by using with the spiking method, was selected for the detection of UA in human urine samples. Urine samples were collected from 5 different healthy adults as control measurements with a non-bias prior to medical diagnosis. The urine sample was diluted with 0.1 M of PBS solution (pH 6) in a ratio of 1:1. Known amounts of UA (0.5, 1.0 and 2.0 mM) were added to the diluted samples. 40 µL of the prepared samples were analyzed using the cotton thread sensor via DPV. The DPV results were compared to the values obtained with a LDI-MS (Autoflex III MALDI-TOF mass spectrometer; Bruker, MA, USA). For the LDI-MS analysis, 10 µL spiked samples were dropped on a stainless-steel MALDI-MS target plate and dried at room temperature (25 ± 5°C) prior to analysis by LDI-MS.

The electrochemical sensor was also integrated into a diaper and used for the detection of UA in artificial urine. The artificial urine solution was prepared as described in a previous report (Hiraoka et al. 2020) with UA concentrations (1–3 mM).

3. Results And Discussion

3.1 Physical characterization of cotton thread-based electrode

The surface of the cotton thread working electrode was characterized by scanning electron microscopy (SEM) with an energy dispersive X-rays spectroscopy (EDX) as shown in Fig. 1. SEM images display a smooth morphology for the uncoated cotton thread, whereas the carbon-coated cotton thread show higher surface roughness. To increase the specific surface area and electrical conductivity of the cotton thread, gold nanoparticles (AuNPs) were added via electrodeposition. SEM images show that the AuNPs were uniformly deposited on the cotton thread surface of the carbon-coated cotton thread surface, with a particle size varying between 98.10 and 100.42 nm. EDX measurements were used to identify the characteristic peaks of Au as shown in Fig. 1d. The weight contents of C, O and Au were 74.59%, 1.59% and 23.82%, and the atom content of C, O and Au were 96.57%, 1.55% and 1.88%.

3.2 Fabrication of the modified cotton thread-based sensor

A two-step fabrication was carried out to create the AuNPs/carbon-coated cotton thread working electrode. Initially, cotton threads were soaked in carbon ink and passed through a pinhole to create the uniformed coating on the cotton thread's surface and remove the excess amount of the carbon ink. $HAuCl_4 \cdot 3H_2O$ was electrodeposited to form AuNPs onto the carbon-coated cotton thread. Several parameters affecting the electrochemical performance of the sensor were optimized, such as the $HAuCl_4 \cdot 3H_2O$ concentration and the electrodeposition time measuring by DPV in 1.0 mM UA.

The effect of $HAuCl_4 \cdot 3H_2O$ concentration on the sensitivity of the sensor was systematically investigated as shown in Fig. 2a and b. Five different concentrations of $HAuCl_4 \cdot 3H_2O$ were electrodeposited on the surface of the sensor at a deposition potential of −0.6 V for 120 s. The results show that the anodic peak current response increased with the increasing concentration of $HAuCl_4 \cdot 3H_2O$, and the highest anodic peak current was obtained at a concentration of 3.0 mM. After reaching the maximum, the anodic current responses decreased for concentrations higher than 3.0 mM due to the higher density of gold cluster causing the agglomeration on the thread's surface (Fig. S1). Agglomeration leads to a decreased surface area and smaller electrochemical response of the system. We selected a concentration of 3.0 mM $HAuCl_4 \cdot 3H_2O$ at 3.0 for the modification of the thread-based sensor.

The effect of electrodeposition time was also investigated in a range between 30 and 240 s. As shown in Fig. 2c and 2d, the anodic peak current increased when the electrodeposition time increased, and the

highest anodic peak current was obtained at 120 s of deposition time. After the maximum is reached, we found that the anodic peak current response decreased with increasing electrodeposition time. Longer electrodeposition times mean denser gold clusters (Fig. S2) hence leading to the decreasing of surface area. 120 seconds was chosen as the electrodeposition time for further experiments.

3.3 Electrochemical characterization of the sensor

The electrochemical behavior of the carbon-coated cotton thread, with and without AuNPs, was investigated by cyclic voltammetry (CV), using 5.0 mM $[Fe(CN)_6]^{3-/4-}$ in 0.1 M KCl as shown in Fig. 3a. In the cyclic voltammograms, the presence of AuNPs on the carbon-coated cotton thread (green line), showed higher anodic and cathodic peak currents towards $[Fe(CN)_6]^{3-/4-}$ detection, which was approximately 2 times higher than the current for the thread absent of AuNPs (pink line). The incorporation of AuNPs on the surface improves both the specific surface area and the electrochemical conductivity of the sensor, hence leading to improved sensitivity.

To assess the analytical performance of the sensor, 1.0 mM UA was measured using differential pulse voltammetry (DPV) as shown in Fig. 3b. The anodic peak current response for UA measured on the AuNPs/carbon-coated cotton thread (yellow line) significantly increased compared to the one measured on the carbon-coated cotton thread (blue line). These results indicated that the presence of AuNPs can enhance the electrochemical response for UA detection. Electrochemical impedance spectroscopy (EIS) was also used to confirm the enhanced sensitivity of AuNPs modified cotton thread-based electrodes. As shown in Fig. 3c, the smallest semicircle was observed for the AuNPs modified cotton thread-based sensor. The low charge transfer resistance occurred because the AuNPs modified electrodes (blue) can effectively accelerate the electron transfer through cotton thread-based electrode surface. The cotton thread-based sensor (orange) shows the higher R_{ct} value which indicated a higher electron transfer resistance, hence indicating that the AuNP coated electrode was a suitable working electrode for UA detection.

3.4 Optimization of parameters for uric acid detection

To obtain the highest electrochemical sensitivity of the developed sensor for UA, electrochemical parameters such as step potential, amplitude and pulse width were systematically optimized when measuring 1.0 mM UA in 0.1 M PBS. The selection of optimal conditions was based on the highest current response along with the smaller peak width and high peak symmetry. Fig. S3 shows that the highest anodic peak current response at 15 mV of step potential, an amplitude of 200 mV, and a pulse width of 50 mV. At higher values of step potential, amplitude and pulse width, the anodic peak current response decreased due to broader peak shape. Therefore, in this study the above-mentioned conditions were selected for the detection of UA.

3.5 The analytical performance of the cotton thread-based sensor

The analytical performance of the AuNPs modified cotton thread-based sensor on the detection of UA was investigated via DPV. As shown in Fig. 4, the anodic peak current linearly increased with UA concentration in the range between 10 µM and 5.0 mM (Fig. 4a). Two linear ranges of UA were observed from 10 µM–0.5 mM (Fig. 4b) and 0.5–5.0 mM (Fig. 4c) with a correlation coefficient (R^2) of 0.9975 and 0.9987. The limit of detection (LOD) was calculated using the following equation: LOD = 3S/N, where S is a standard deviation of a signal obtained from a blank solution (n = 7), and N is a slope of calibration curve. The LOD of AuNPs modified cotton thread-based sensor was found to be 0.12 µM.

A linear range of 0.1–2.0 mM was obtained when Au NPs were not present on the surface of the electrode (Fig. S4) which is a narrower range than that of 10 µM to 5.0 mM for the sensor coated with AuNPs (Fig. 4). These results confirm that the presence of AuNPs is improves the sensor's signal linearity possibly due to the enhanced surface area and conductivity of the AuNPs. The slope of the calibration curve obtained from the sensor coated with AuNPs was higher than the slope for the sensor without AuNPs (Fig. S4), suggesting that the enhanced sensor sensitivity results from the presence of AuNPs. Interestingly, LOD of the carbon-coated cotton thread-based sensor was found approximately 13 times higher than the sensor with AuNPs (0.12 µM). These results indicate that the presence of AuNPs on the electrode's surface drastically improved the overall analytical performance of the sensor.

Our sensor has a lower LOD and wider linear range than those previously reported as summarized in Table 1.

Table 1
Comparison of non-enzymatic determination of UA using different modified electrodes.

Chemically Modified electrode	Method	LOD (μM)	Linear range (μM)	Refs.
MoS_2 based flexible sensor	Amperometry	1.169	10–400	(Sha et al. 2019)
H-Fe_3O_4@C/GNS/GCE	DPV	0.41	1–100	(Song et al. 2017)
RGO/poly-l-lysine/GCE	DPV	0.15	20–200	(Zhang et al. 2017)
Poly (DPA)/SiO_2@Fe_3O_4/CPE	DPV	0.40	1.2–8.2	(Veera Manohara Reddy et al. 2018)
Au-Cu_2O/rGO/GCE	DPV	6.5	100–900	(Aparna et al. 2018)
GNP/ITO	DPV	0.28	10–100	(Rahman et al. 2017)
Pd/rGO/GCE	DPV	1.6	6–469.5	(Wang et al. 2017)
NiO-trGO/GCE	DPV	10	100–500	(Aparna and Sivasubramanian 2018)
Tin-rGO/GCE	DPV	0.35	30–215	(Feng et al. 2019)
AuNPs/cotton thread-based sensor	DPV	0.12	10–5000	This work

Abbreviations: DPV, differential pulse voltammetry; MoS_2, molybdenum disulfide; H-Fe_3O_4, hallow magnetite; C, carbon; GNS, graphene oxide nanosheets; GCE, glassy carbon electrode; RGO, reduced graphene oxide; DPA, dipicolinic acid; CPE, carbon paste electrode; Cu_2O, cuprous oxide; GNP, graphene nanoplatelet; ITO, tin oxide electrode; Pd, palladium; NiO, nickel oxide; trGO, thermally reduced graphene oxide; Tin, titanium nitride; AuNPs, gold nanoparticles.

3.6 Interference study

The anti-interference ability of the cotton thread-based sensor was assessed by adding potential interfering substances such as a 10-fold excess of glucose, creatinine, KCl, NaCl, urea, and a 1-fold excess of ascorbic acid and 1% excess of BSA. As shown in Fig. 5, there was no significant changes in the current measurements as the result of the presence of interfering substances.

3.7 Stability of the cotton thread-based sensor

The stability of the cotton thread-based sensor was investigated by measuring the DPV response to 1.0 mM of UA in PBS solution multiple times. The sensors were stored at room temperature for 30 days and the current responses remained above 96.48% of their initial values as shown in Fig. S5. These results are evidence of the stability and reproducibility of our sensors.

3.8 Real—life sample application and method validation

To confirm the potential application of the cotton thread-based sensor in complex biological matrices, pooled urine serum samples were collected from 5 healthy adults (female) to represent non-bias errors

prior to medical diagnosis. Each urine sample was diluted with 0.1 M PBS solution, pH 6.5 (1:1). The cotton thread-based sensor was used to detect UA in the samples via a standard addition method. A known amount of UA (0.5, 1.0 and 2.0 mM) was added to the diluted samples. The analytical results are summarized in Table 2. The percent recovery ranged from 100 to 108 with a relative standard derivation (RSD) of less than 6.0% (n = 3). These results were validated by comparing these measurements with those obtained with a standard LDI-MS method as shown in Table 2.

Table 2
Determination of UA in human urine samples using the modified cotton thread-based sensor and LDI-MS (n = 3).

Spiked UA concentration (mM)	Modified cotton thread- based sensor (mM)	Standard LDI-MS (mM)	Recovery (%)
Blank	0.61 ± 0.08	0.70 ± 0.09	–
0.5	1.11 ± 0.02	1.17 ± 0.05	100
1.0	1.69 ± 0.05	1.73 ± 0.07	108
2.0	2.77 ± 0.12	2.84 ± 0.15	108

The cotton thread-based electrochemical sensor was also used to detect UA in artificial urine media. As shown in Fig. S6, a linearity was found in a range of 0.4–3.4 mM for UA in artificial urine samples. The sensor threads were directly integrated into a diaper and used to measure UA in artificial urine poured over the diaper. Known concentrations of UA (1.0, 2.0 and 3.0 mM) were added to the artificial urine media, and 50 mL of the solution were poured into the diaper. Table S1 summarizes the recovery percentages which ranged from 96 to 105 with an RSD of less than 9% (n = 3), verifying the high accuracy of the sensor in the diaper.

4. Conclusions

An electrochemical sensor for the non-enzymatic detection of UA, was fabricated using cotton threads coated with AuNPs. The cotton thread-based sensor exhibited high sensitivity to UA. The sensor shows a wide linear detection range of 10 µM−5.0 mM with a low detection limit of 0.12 µM. This enzyme-free sensor exhibits long-term stability, anti-interference ability, and satisfactory recoveries for detecting UA in human urine samples. The sensor was effectively applied for differentiation between a patient diagnosed with gout and a normal individual with a required cut off value (uric acid ≥ 4.46 mM). This sensing platform was successfully integrated into a diaper for direct detection of UA in artificial urine, enabling its potential for gout disease screening.

Declarations

Acknowledgement

This research was supported by the Ratchadapisek Sompoch Endowment Fund (2019), Chulalongkorn University (761002) and TSRI Fund (CU_FRB640001_01_62_1).

Authors' contributions

KT Methodology and Writing-original draft preparation, NR Investigation and Editing-original draft preparation, OC Supervision and Funding acquisition, NR Conceptualization, Project administration and Writing-Review and Editing

Conflict of interest

The authors declare no conflict of interest.

Declaration section

All procedures performed in studies involving human participants were in accordance with the ethical standards of the institutional research committee from Chulalongkorn Hospital.

References

Ahmed NM, Sabah FA, Kabaa EA, Zar Myint MT (2019) Single- and double-thread activated carbon fibers for pH sensing. Mate Chem Phys 221:288-294. http://doi.org:10.1016/j.matchemphys.2018.09.059

Anastasova S, Crewther B, Bembnowicz P, Curto V, Ip HM, Rosa B, Yang GZ (2017) A wearable multisensing patch for continuous sweat monitoring. Biosens Bioelectron 93:139-145. http://doi.org:10.1016/j.bios.2016.09.038

Aparna T, Sivasubramanian R (2018) A facile hydrothermal synthesis of three dimensional flower-like NiO-thermally reduced graphene oxide (trGO) nanocomposite for selective determination of dopamine in presence of uric acid and ascorbic acid. J Nanosci Nanotech 18 (2):789-797

Aparna TK, Sivasubramanian R, Dar MA (2018) One-pot synthesis of Au-Cu2O/rGO nanocomposite based electrochemical sensor for selective and simultaneous detection of dopamine and uric acid. J Alloys Compd 741:1130-1141. http://doi.org:10.1016/j.jallcom.2018.01.205

Arora K, Tomar M, Gupta V (2014) Effect of processing parameters for electrocatalytic properties of SnO(2) thin film matrix for uric acid biosensor. Analyst 139 (4):837-849. http://doi.org:10.1039/c3an01582c

Azmi NE, Ramli NI, Abdullah J, Abdul Hamid MA, Sidek H, Abd Rahman S, Ariffin N, Yusof NA (2015) A simple and sensitive fluorescence based biosensor for the determination of uric acid using H2O2-sensitive quantum dots/dual enzymes. Biosens Bioelectron 67:129-133. http://doi.org:10.1016/j.bios.2014.07.056

Azmi NE, Rashid AHA, Abdullah J, Yusof NA, Sidek H (2018) Fluorescence biosensor based on encapsulated quantum dots/enzymes/sol-gel for non-invasive detection of uric acid. J Lumin 202:309-315. http://doi.org:10.1016/j.jlumin.2018.05.075

Bai Z, Zhou C, Xu H, Wang G, Pang H, Ma H (2017) Polyoxometalates-doped Au nanoparticles and reduced graphene oxide: A new material for the detection of uric acid in urine. Sens Actuators B Chem 243:361-371. http://doi.org:10.1016/j.snb.2016.11.159

Bandodkar AJ, Hung VW, Jia W, Valdes-Ramirez G, Windmiller JR, Martinez AG, Ramirez J, Chan G, Kerman K, Wang J (2013) Tattoo-based potentiometric ion-selective sensors for epidermal pH monitoring. Analyst 138 (1):123-128. http://doi.org:10.1039/c2an36422k

Caldara M, Colleoni C, Guido E, Re V, Rosace G (2016) Optical monitoring of sweat pH by a textile fabric wearable sensor based on covalently bonded litmus-3-glycidoxypropyltrimethoxysilane coating. Sens Actuators B Chem 222:213-220

Charoenkitamorn K, Chailapakul O, Siangproh W (2015) Development of gold nanoparticles modified screen-printed carbon electrode for the analysis of thiram, disulfiram and their derivative in food using ultra-high performance liquid chromatography. Talanta 132:416-423. http://doi.org:10.1016/j.talanta.2014.09.020

da Cruz FS, Paula FdS, Franco DL, dos Santos WTP, Ferreira LF (2017) Electrochemical detection of uric acid using graphite screen-printed electrodes modified with Prussian blue/poly(4-aminosalicylic acid)/Uricase. J Electroanal Chem 806:172-179. http://doi.org:10.1016/j.jelechem.2017.10.070

Doménech-Carbó A, Pontones JL, Doménech-Casasús C, Artés J, Villaroya S, Ramos D (2018) Electrochemical detection and screening of bladder cancer recurrence using direct electrochemical analysis of urine: A non-invasive tool for diagnosis. Sens Actuators B Chem 265:346-354. http://doi.org:10.1016/j.snb.2018.03.048

Eftekhari A, Hasanzadeh M, Sharifi S, Dizaj SM, Khalilov R, Ahmadian E (2019) Bioassay of saliva proteins: The best alternative for conventional methods in non-invasive diagnosis of cancer. Int J Biol Macromol 124:1246-1255. http://doi.org:10.1016/j.ijbiomac.2018.11.277

Feng J, Li Q, Cai J, Yang T, Chen J, Hou X (2019) Electrochemical detection mechanism of dopamine and uric acid on titanium nitride-reduced graphene oxide composite with and without ascorbic acid. Sens Actuators B Chem 298:126872. http://doi.org:10.1016/j.snb.2019.126872

Hiraoka R, Kuwahara K, Wen YC, Yen TH, Hiruta Y, Cheng CM, Citterio D (2020) Paper-Based Device for Naked Eye Urinary Albumin/Creatinine Ratio Evaluation. ACS Sens 5 (4):1110-1118. http://doi.org:10.1021/acssensors.0c00050

Income K, Ratnarathorn N, Khamchaiyo N, Srisuvo C, Ruckthong L, Dungchai W (2019) Disposable Nonenzymatic Uric Acid and Creatinine Sensors Using muPAD Coupled with Screen-Printed Reduced Graphene Oxide-Gold Nanocomposites. Int J Anal Chem 2019:3457247. http://doi.org:10.1155/2019/3457247

Ji D, Liu Z, Liu L, Low SS, Lu Y, Yu X, Zhu L, Li C, Liu Q (2018) Smartphone-based integrated voltammetry system for simultaneous detection of ascorbic acid, dopamine, and uric acid with graphene and gold nanoparticles modified screen-printed electrodes. Biosens Bioelectron 119:55-62. http://doi.org:10.1016/j.bios.2018.07.074

Jia W, Bandodkar AJ, Valdes-Ramirez G, Windmiller JR, Yang Z, Ramirez J, Chan G, Wang J (2013) Electrochemical tattoo biosensors for real-time noninvasive lactate monitoring in human perspiration. Anal Chem 85 (14):6553-6560. http://doi.org:10.1021/ac401573r

Li T, Zou L, Zhang J, Li G, Ling L (2019) Non-invasive diagnosis of bladder cancer by detecting telomerase activity in human urine using hybridization chain reaction and dynamic light scattering. Anal Chim Acta 1065:90-97. http://doi.org:10.1016/j.aca.2019.03.039

Li XL, Li G, Jiang YZ, Kang D, Jin CH, Shi Q, Jin T, Inoue K, Todoroki K, Toyo'oka T, Min JZ (2015) Human nails metabolite analysis: A rapid and simple method for quantification of uric acid in human fingernail by high-performance liquid chromatography with UV-detection. J Chromatogr B Analyt Technol Biomed Life Sci 1002:394-398. http://doi.org:10.1016/j.jchromb.2015.08.044

Liu L, Liu L, Wang Y, Ye BC (2019) A novel electrochemical sensor based on bimetallic metal-organic framework-derived porous carbon for detection of uric acid. Talanta 199:478-484. http://doi.org:10.1016/j.talanta.2019.03.008

Liu P, Pan W, Liu Y, Liu J, Xu W, Guo X, Liu C, Zhang Y, Ge Y, Huang Y (2018) Fully flexible strain sensor from core-spun elastic threads with integrated electrode and sensing cell based on conductive nanocomposite. Compos Sci Technol 159:42-49. http://doi.org:10.1016/j.compscitech.2018.02.034

Liu X, Lillehoj PB (2017) Embroidered electrochemical sensors on gauze for rapid quantification of wound biomarkers. Biosens Bioelectron 98:189-194. http://doi.org:10.1016/j.bios.2017.06.053

Liu X, Xie L, Li H (2012) Electrochemical biosensor based on reduced graphene oxide and Au nanoparticles entrapped in chitosan/silica sol–gel hybrid membranes for determination of dopamine and uric acid. J Electroanal Chem 682:158-163. http://doi.org:10.1016/j.jelechem.2012.07.031

Martin A, Kim J, Kurniawan JF, Sempionatto JR, Moreto JR, Tang G, Campbell AS, Shin A, Lee MY, Liu X, Wang J (2017) Epidermal Microfluidic Electrochemical Detection System: Enhanced Sweat Sampling and Metabolite Detection. ACS Sens 2 (12):1860-1868. http://doi.org:10.1021/acssensors.7b00729

Michelena J, Alonso C, Martinez-Arranz I, Altamirano J, Mayo R, Sancho-Bru P, Bataller R, Gines P, Castro A, Caballeria J (2019) Metabolomics Discloses a New Non-invasive Method for the Diagnosis and Prognosis of Patients with Alcoholic Hepatitis. Ann Hepatol 18 (1):144-154. http://doi.org:10.5604/01.3001.0012.7906

Oliveira MC, Watanabe EY, Agustini D, Banks CE, Marcolino-Júnior LH, Bergamini MF (2019) Nonenzymatic sensor for determination of glucose in blood plasma based on nickel oxyhydroxide in a microfluidic system of cotton thread. J Electroanal Chem 840:153-159. http://doi.org:10.1016/j.jelechem.2019.03.038

Polanský R, Soukup R, Řeboun J, Kalčík J, Moravcová D, Kupka L, Švantner M, Honnerová P, Hamáček A (2017) A novel large-area embroidered temperature sensor based on an innovative hybrid resistive thread. Sensor Actuat A-Phys 265:111-119. http://doi.org:10.1016/j.sna.2017.08.030

Pormsila W, Krahenbuhl S, Hauser PC (2009) Capillary electrophoresis with contactless conductivity detection for uric acid determination in biological fluids. Anal Chim Acta 636 (2):224-228. http://doi.org:10.1016/j.aca.2009.02.012

Promphet N, Rattanawaleedirojn P, Siralertmukul K, Soatthiyanon N, Potiyaraj P, Thanawattano C, Hinestroza JP, Rodthongkum N (2019) Non-invasive textile based colorimetric sensor for the simultaneous detection of sweat pH and lactate. Talanta 192:424-430. http://doi.org:10.1016/j.talanta.2018.09.086

Rahman MM, Lopa NS, Ju MJ, Lee J-J (2017) Highly sensitive and simultaneous detection of dopamine and uric acid at graphene nanoplatelet-modified fluorine-doped tin oxide electrode in the presence of ascorbic acid. J Electroanal Chem 792:54-60. http://doi.org:10.1016/j.jelechem.2017.03.038

Reches M, Mirica KA, Dasgupta R, Dickey MD, Butte MJ, Whitesides GM (2010) Thread as a matrix for biomedical assays. ACS Appl Mater Interfaces 2 (6):1722-1728. http://doi.org:10.1021/am1002266

Ren J, Wang C, Zhang X, Carey T, Chen K, Yin Y, Torrisi F (2017) Environmentally-friendly conductive cotton fabric as flexible strain sensor based on hot press reduced graphene oxide. Carbon 111:622-630. http://doi.org:10.1016/j.carbon.2016.10.045

Ruecha N, Lee J, Chae H, Cheong H, Soum V, Preechakasedkit P, Chailapakul O, Tanev G, Madsen J, Rodthongkum N, Kwon O-S, Shin K (2017) Paper-Based Digital Microfluidic Chip for Multiple Electrochemical Assay Operated by a Wireless Portable Control System. Adv Mater Technol 2 (3):1600267. http://doi.org:10.1002/admt.201600267

Sha R, Vishnu N, Badhulika S (2019) MoS2 based ultra-low-cost, flexible, non-enzymatic and non-invasive electrochemical sensor for highly selective detection of Uric acid in human urine samples. Sens Actuators B Chem 279:53-60. http://doi.org:10.1016/j.snb.2018.09.106

Song H, Xue G, Zhang J, Wang G, Ye B-C, Sun S, Tian L, Li Y (2017) Simultaneous voltammetric determination of dopamine and uric acid using carbon-encapsulated hollow Fe3O4 nanoparticles anchored to an electrode modified with nanosheets of reduced graphene oxide. Microchim Acta 184 (3):843-853. http://doi.org:10.1007/s00604-016-2067-1

Veera Manohara Reddy Y, Sravani B, Agarwal S, Gupta VK, Madhavi G (2018) Electrochemical sensor for detection of uric acid in the presence of ascorbic acid and dopamine using the poly(DPA)/SiO 2 @Fe 3 O 4 modified carbon paste electrode. J Electroanal Chem 820:168-175. http://doi.org:10.1016/j.jelechem.2018.04.059

Wang H, Xiao L-G, Chu X-F, Chi Y-D, Yang X-T (2016) Rational Design of Gold Nanoparticle/graphene Hybrids for Simultaneous Electrochemical Determination of Ascorbic Acid, Dopamine and Uric Acid. Chinese J Anal Chem 44 (12):e1617-e1625. http://doi.org:10.1016/s1872-2040(16)60983-0

Wang J, Yang B, Zhong J, Yan B, Zhang K, Zhai C, Shiraishi Y, Du Y, Yang P (2017) Dopamine and uric acid electrochemical sensor based on a glassy carbon electrode modified with cubic Pd and reduced graphene oxide nanocomposite. J Colloid Interface Sci 497:172-180. http://doi.org:10.1016/j.jcis.2017.03.011

Wang Z, Guo H, Gui R, Jin H, Xia J, Zhang F (2018) Simultaneous and selective measurement of dopamine and uric acid using glassy carbon electrodes modified with a complex of gold nanoparticles and multiwall carbon nanotubes. Sens Actuators B Chem 255:2069-2077. http://doi.org:10.1016/j.snb.2017.09.010

Weng X, Kang Y, Guo Q, Peng B, Jiang H (2019) Recent advances in thread-based microfluidics for diagnostic applications. Biosens Bioelectron 132:171-185. http://doi.org:10.1016/j.bios.2019.03.009

Yang F, Yu Z, Li X, Ren P, Liu G, Song Y, Wang J (2018) Design and synthesis of a novel lanthanide fluorescent probe (Tb(III)-dtpa-bis(2,6-diaminopurine)) and its application to the detection of uric acid in urine sample. Spectrochim Acta A Mol Biomol Spectrosc 203:461-471. http://doi.org:10.1016/j.saa.2018.06.011

Yukird J, Kongsittikul P, Qin J, Chailapakul O, Rodthongkum N (2018) ZnO@graphene nanocomposite modified electrode for sensitive and simultaneous detection of Cd (II) and Pb (II). Synth Met 245:251-259. http://doi.org:10.1016/j.synthmet.2018.09.012

Zhang D, Li L, Ma W, Chen X, Zhang Y (2017) Electrodeposited reduced graphene oxide incorporating polymerization of l-lysine on electrode surface and its application in simultaneous electrochemical determination of ascorbic acid, dopamine and uric acid. Mater Sci Eng C Mater Biol Appl 70 (Pt 1):241-249. http://doi.org:10.1016/j.msec.2016.08.078

Figures

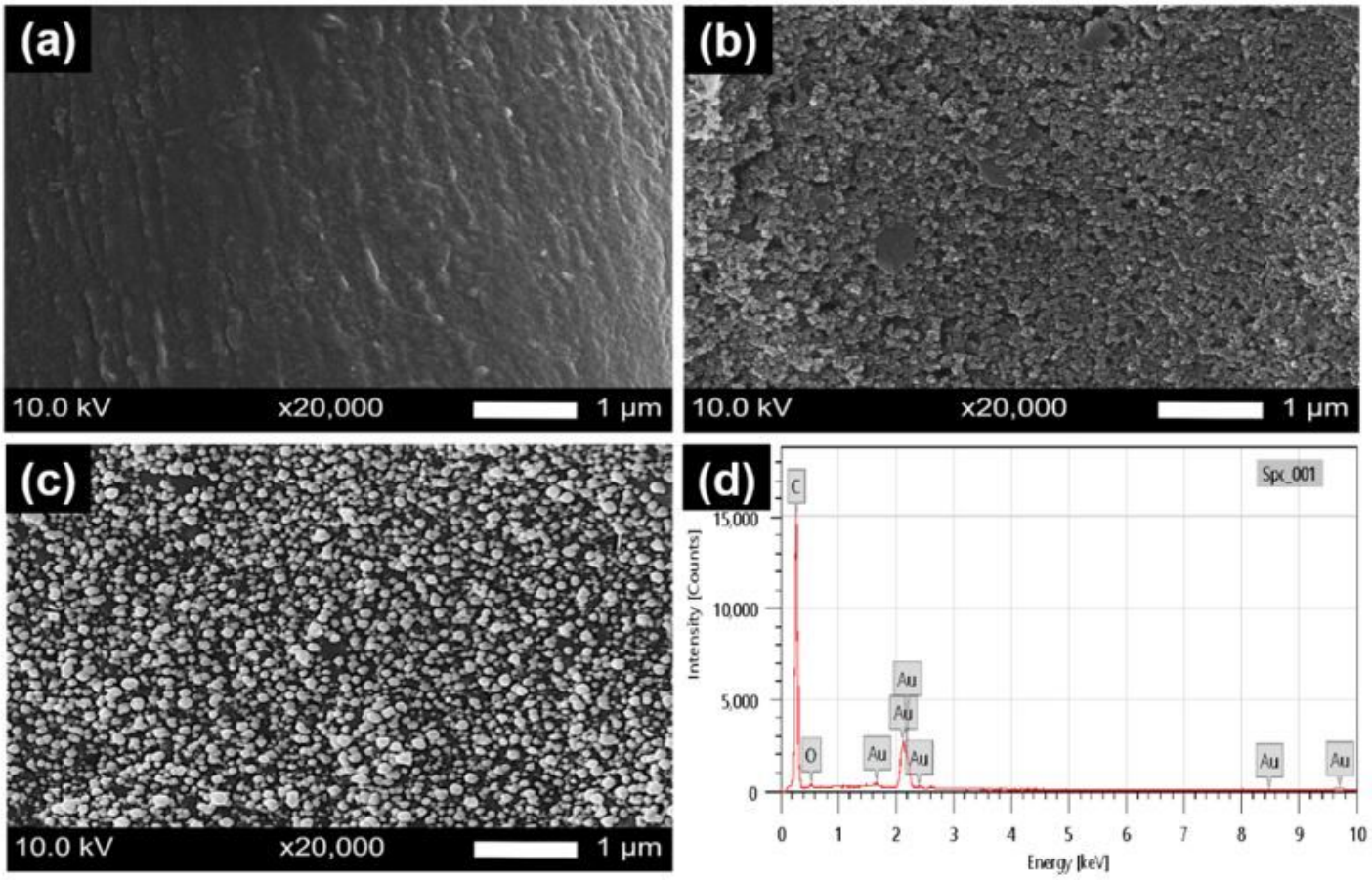

Figure 1

SEM images of (a) uncoated cotton thread, (b) carbon-coated cotton thread, (c) AuNPs modified carbon-coated cotton thread with magnification of 20,000×, and (d) SEM-EDX spectrum of AuNPs modified carbon-coated cotton thread surface.

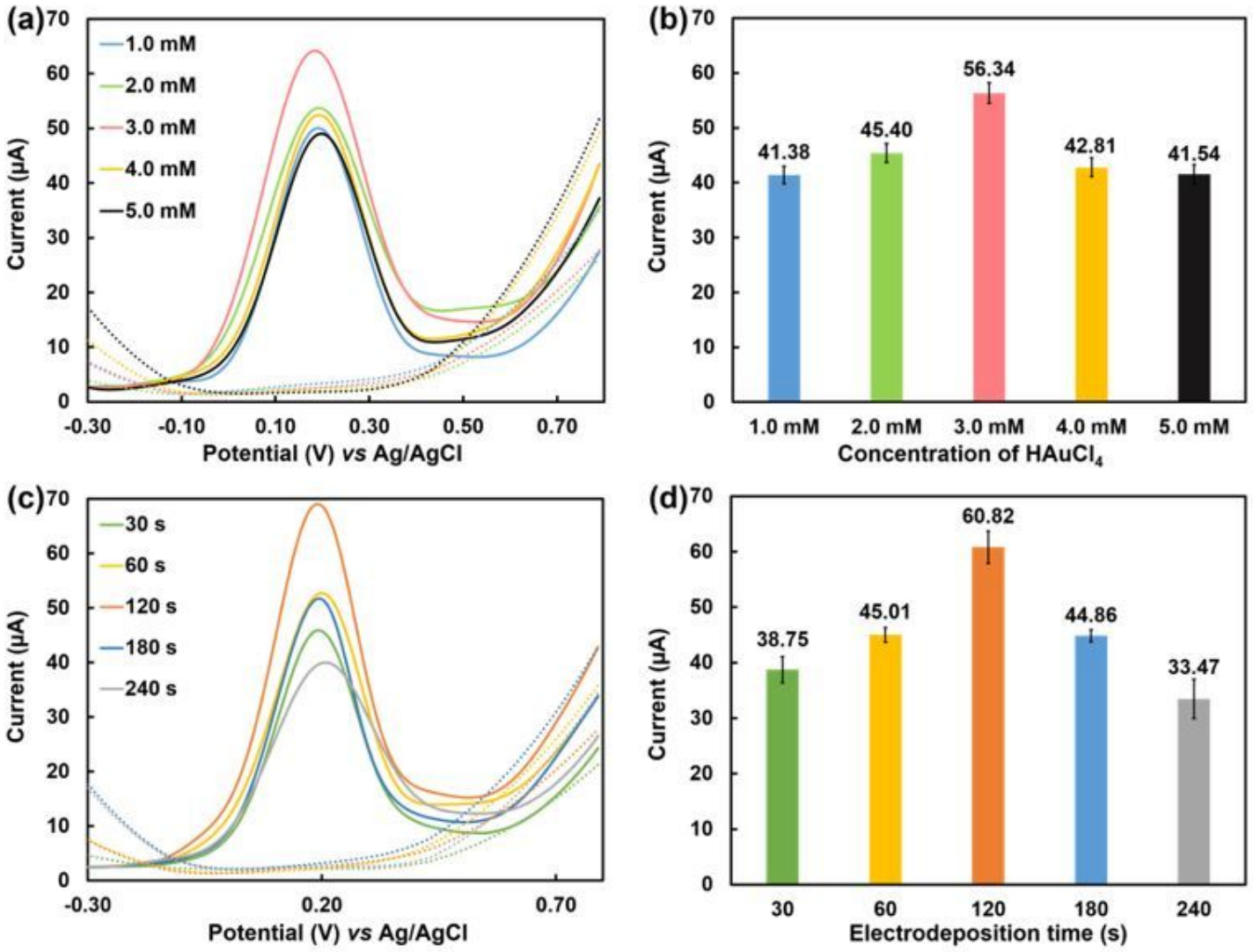

Figure 2

Differential pulse voltammograms of 1.0 mM UA (solid lines) and 0.1 M PBS (dotted lines) using AuNPs/carbon-coated cotton thread with different (a) concentrations of HAuCl4·3H2O (1.0, 2.0, 3.0, 4.0 mM and 5.0 mM) and (c) electrodeposition times (30, 60, 120, 180 and 240 s) for AuNPs deposited on the cotton thread-based electrochemical sensor, and anodic peak currents obtained from differential pulse voltammograms in (b) Fig. 2a and (d) Fig. 2c by measurements using 3 individual single-use electrodes (n=3).

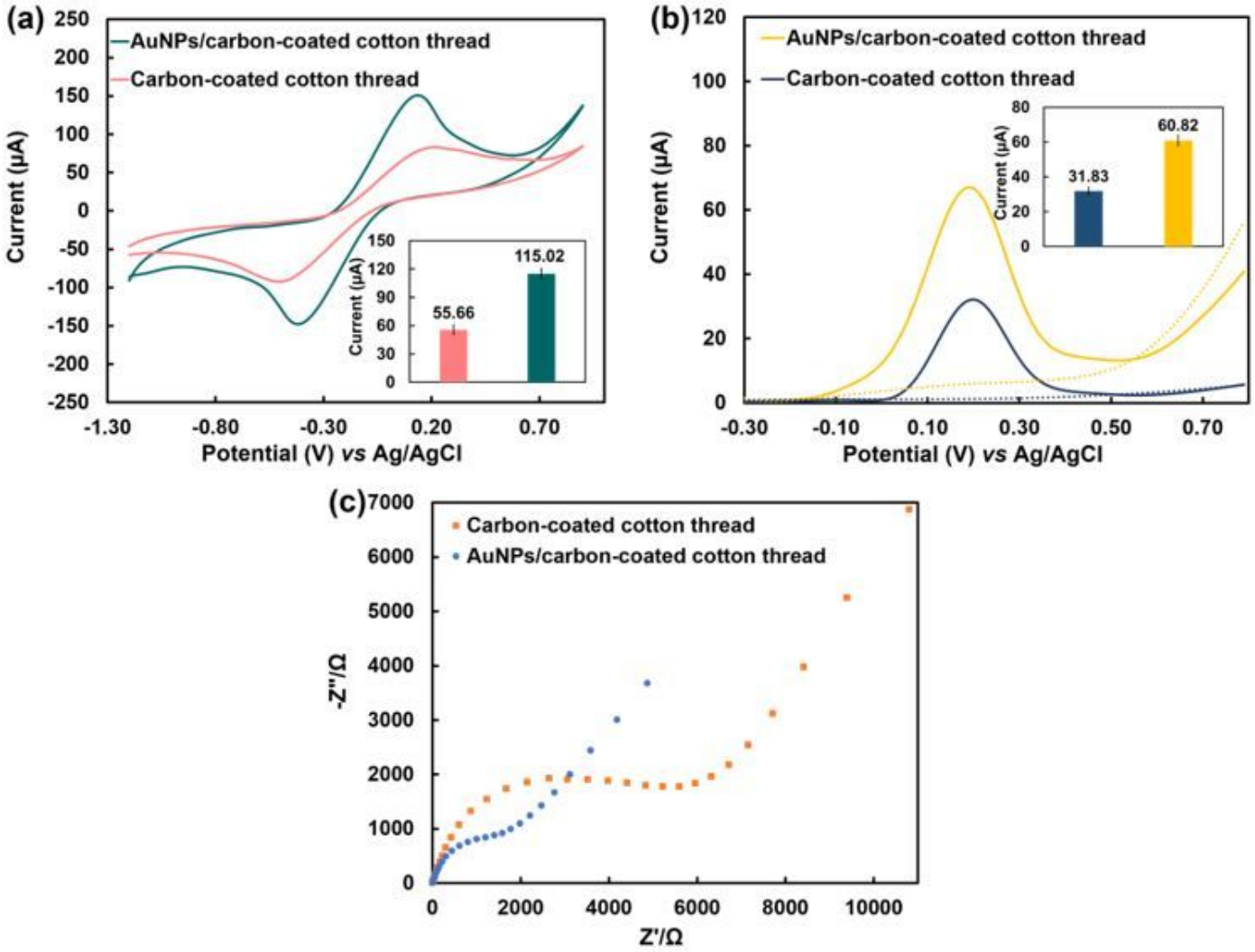

Figure 3

(a) Cyclic voltammograms of 5.0 mM [Fe(CN)6] 3−/4− on AuNPs/carbon-coated cotton thread and carbon-coated cotton thread with a scan rate of 100 mV/s, and the anodic peak currents obtained from cyclic voltammograms (inset), (b) Differential pulse voltammograms of 1.0 mM UA (solid lines) and 0.1 M PBS (dotted lines) on AuNPs/carbon-coated cotton thread and carbon-coated cotton thread, and the anodic peak currents obtained from differential pulse voltammograms (inset) and (c) Nyquist plots of 2.0 mM [Fe(CN)6]3−/4− measured on carbon-coated cotton thread and AuNPs/carbon-coated cotton thread-based electrodes.

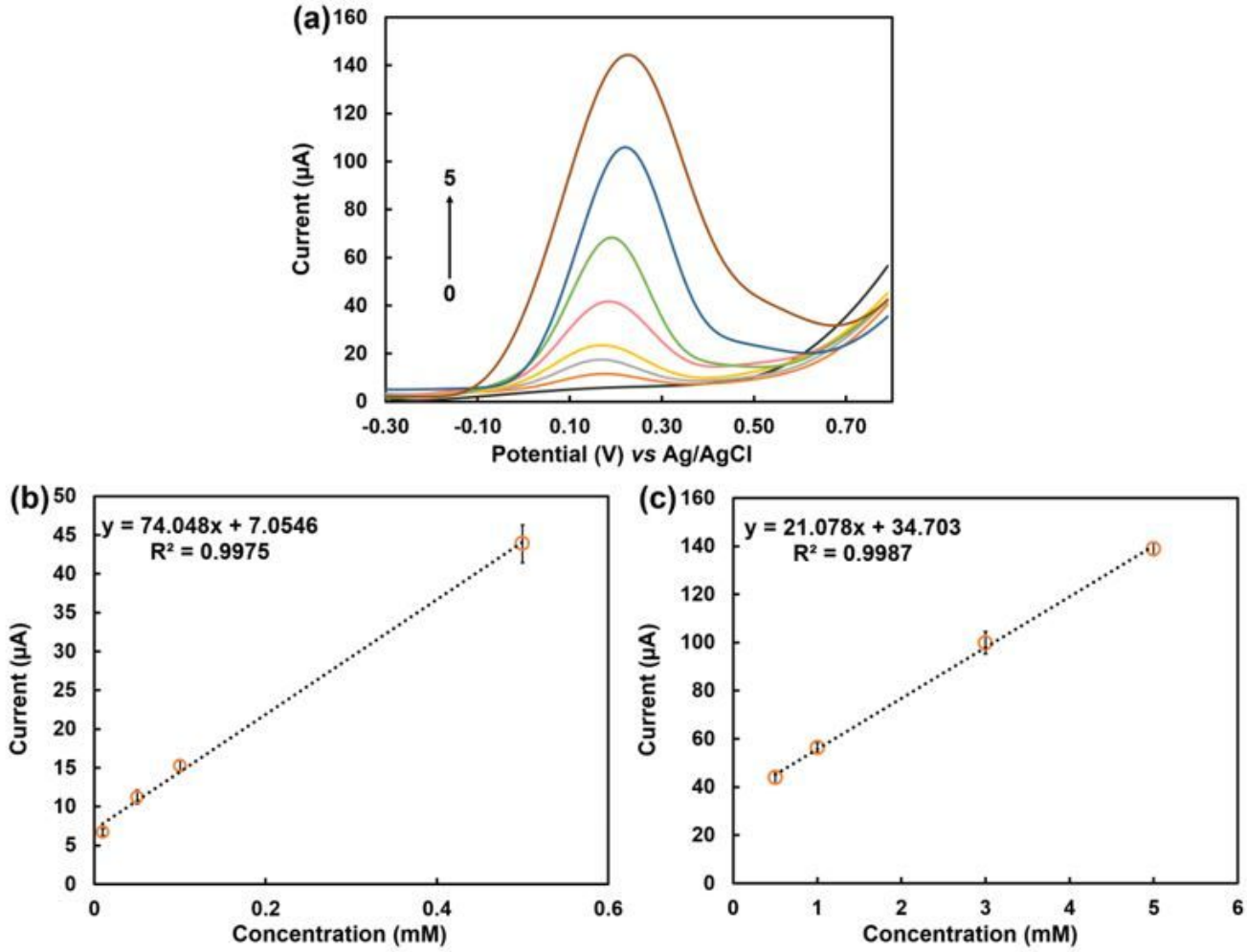

Figure 4

(a) Differential pulse voltammograms of different concentrations of UA (0-5 mM) on the modified cotton thread-based sensor and linearities ranging from (b) 10 μM-0.5 mM and (c) 0.5-5.0 mM by measurements using 3 individual single-use electrodes (n=3).

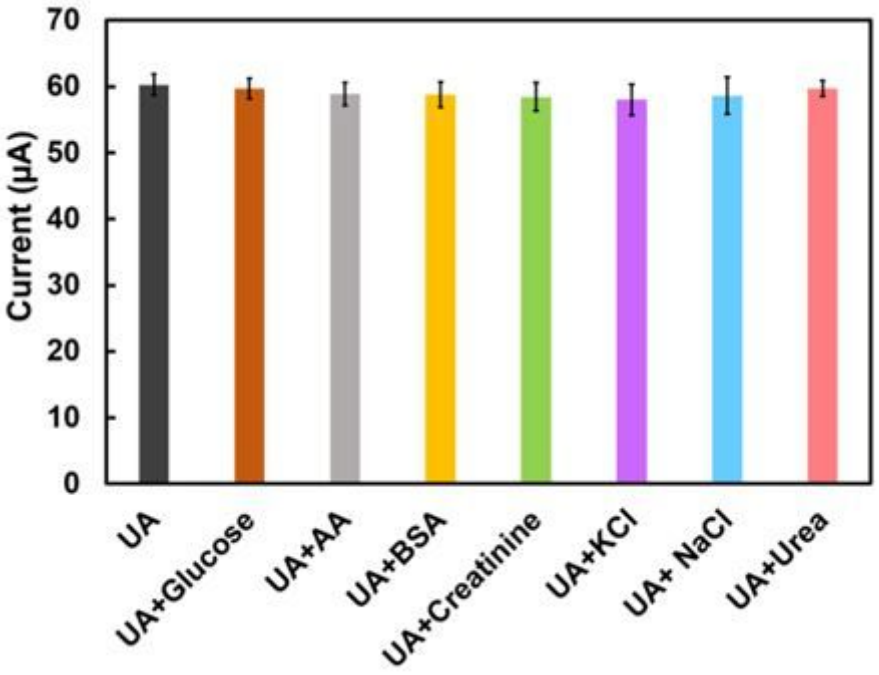

Figure 5

Current responses towards 1.0 mM UA on the cotton thread-based sensor in the absence and presence of several interferences by measurements using 3 individual single-use electrodes (n=3).

Supplementary Files

This is a list of supplementary files associated with this preprint. Click to download.

- SIofManuscript04152021.docx